Magn Reson Med Sci 2022; 21; 29–40
doi:10.2463/mrms.rev.2021-0052 Published Online: September 1, 2021

REVIEW

An Invited Review for the Special 20th Anniversary Issue of MRMS

Review of Quantitative Knee Articular Cartilage MR Imaging

Mai Banjar[1], Saya Horiuchi[2], David N. Gedeon[3], and Hiroshi Yoshioka[3*]

Osteoarthritis (OA) is one of the most prevalent disorders in today's society, resulting in significant socioeconomic costs and morbidity. MRI is widely used as a non-invasive imaging tool for OA of the knee. However, conventional knee MRI has limitations to detect subtle early cartilage degeneration before morphological changes are visually apparent. Novel MRI pulse sequences for cartilage assessment have recently received increased attention due to newly developed compositional MRI techniques, including: T2 mapping, T1rho mapping, delayed gadolinium-enhanced MRI of cartilage (dGEMRIC), sodium MRI, diffusion-weighted imaging (DWI)/ diffusion tensor imaging (DTI), ultrashort TE (uTE), and glycosaminoglycan specific chemical exchange saturation transfer (gagCEST) imaging. In this article, we will first review these quantitative assessments. Then, we will discuss the variations of quantitative values of knee articular cartilage with cartilage layer (depth)- and angle (regional)-dependent approaches. Multiple MRI sequence techniques can discern qualitative differences in knee cartilage. Normal articular hyaline cartilage has a zonal variation in T2 relaxation times with increasing T2 values from the subchondral bone to the articular surface. T1rho values were also higher in the superficial layer than in the deep layer in most locations in the medial and lateral femoral condyles, including the weight-bearing portion. Magic angle effect on T2 mapping is clearly observed in the both medial and lateral femoral condyles, especially within the deep layers. One of the limitations for clinical use of these compositional assessments is a long scan time. Recent new approaches with compressed sensing (CS) and MR fingerprinting (MRF) have potential to provide accurate and fast quantitative cartilage assessments.

Keywords: *quantitative, knee cartilage, magnetic resonance imaging*

Introduction

Osteoarthritis (OA) is the most common type of arthritis, causing tremendous socioeconomic cost and morbidity.[1] Early identification of degenerative changes is important for the treatment of OA. MRI has been widely used as a non-invasive imaging tool for OA of the knee since it was clinically available. Early cartilage MRI studies were focused on signal (contrast) and morphologic changes in cartilage and had been used to detect cartilage surface fraying, fissuring, and cartilage thinning.[2] However, conventional MRI has limitations to detect subtle early cartilage degeneration before morphological changes. In recent decades, quantitative assessment of the biochemical composition of cartilage has been more popular along with advanced MRI techniques and availability of high field magnet such as 3 Tesla (T). In this review article, we first introduce quantitative MRI techniques. Then, variations of quantitative values of knee articular cartilage are reviewed with cartilage layer (depth)- and angle (regional)-dependent approaches, and finally, the recent trends of compositional knee MRI are discussed.

Quantitative Methods of Cartilage MRI

There are novel MRI sequences that characterize and quantify the composition of the hyaline articular cartilage and show promise in the detection of early osteoarthritic changes. These include: T2 mapping, T1rho mapping, sodium imaging, delayed gadolinium-enhanced MRI of cartilage (dGEMRIC), diffusion-weighted imaging (DWI), diffusion

[1]Medical Imaging Department, King Abdullah Medical Complex Jeddah, Jeddah, Saudi Arabia
[2]Department of Radiology, St Luke's International Hospital, Tokyo, Japan
[3]Department of Radiological Sciences, University of California, Irvine, Orange, CA, USA

*Corresponding author: Department of Radiological Sciences, University of California, Irvine, 101, City Drive South, Route 140, Orange, CA 92868, USA, Phone: +1-714-456-8849, Email: hiroshi@hs.uci.edu

Received: April 13, 2021 | Accepted: July 11, 2021

Table 1 Summary of quantitative cartilage MRI

Quantitative cartilage MRI	Associated cartilage contents	Interpretation
T2 mapping	Water, organization of collagen matrix	T2 ↑ = loss of collagen integrity
T1rho mapping	Proteoglycan (GAG), orientation of collagen fiber, concentration of other macromolecules	T1rho ↑ = proteoglycan depletion
dGEMRIC	Proteoglycan (GAG)	T1 ↓ = proteoglycan depletion
Sodium imaging	Proteoglycan (GAG)	Na signal ↓ = proteoglycan depletion, FCD ↓
DWI & DTI	Water molecules, collagen matrix, proteoglycans	ADC signal ↑ = cartilage degeneration
uTE imaging	Water molecules, collagen matrix, proteoglycans	Useful for evaluation of calcified cartilage
gagCEST	Water and proteoglycan (GAG)	gagCEST value ↓ = GAG depletion

ADC, apparent diffusion coefficient; dGEMRIC, delayed gadolinium-enhanced MRI of cartilage; DTI, diffusion tensor imaging; DWI, diffusion-weighted imaging; FCD, fixed charged density; GAG, glycosaminoglycan; gagCEST, glycosaminoglycan specific chemical exchange saturation transfer; uTE, ultrashort TE.

tensor imaging (DTI), ultrashort TE (uTE) imaging, and glycosaminoglycan (GAG) specific chemical exchange saturation transfer (gagCEST). The summary of quantitative cartilage MRI is shown in Table 1.

Biochemical properties of cartilage

Hyaline articular cartilage is composed of four major contents: GAGs (which make up proteoglycans), type II collagen, chondrocytes, and water. Cartilage material contents and orientations vary depending on cartilage zones. The GAG molecules trapped inside the collagen matrix resist compressive loads and generate swelling pressure due to their affinity for water.[3] High GAG content and collagen fiber integrity are essential for the mechanical functions of healthy cartilage. During the early stage of OA, the molecular composition and organization of the extracellular matrix is altered before cartilage fissuring. This progressive disruption of the matrix architecture with loss of GAG and collagen results in poor mechanical function because of a consequent increase in water content.[4,5] These matrix changes are not apparent on conventional morphological MR sequences, while advanced compositional MR imaging techniques provide information on the biochemical properties of cartilage to detect the initial stages of degeneration.

T2 mapping

T2 relaxation time was found to be associated with water content, as well as organization of the collagen matrix.[6–8] An increase in T2 relaxation time correlates with the areas of cartilage damage particularly with loss of the integrity of collagen.[7] While conventional MRI sequences permits subjective evaluation of cartilage signal changes, T2 mapping allows a more objective assessment by generating a grayscale or color map.[9] In order to extract these T2 values from different cartilage compartments, segmentation is required. Calculation of T2 relaxation values from ROI is done by mono-exponential curve fitting of the signal intensity of each voxel.[10,11]

Multiple studies generally demonstrate that T2 mapping shows promise in detecting pre-morphologic stage of OA changes.[12,13] A study by Mosher et al. demonstrated the association between age and higher T2 values in the superficial layer,[14] without a significant gender difference.[11] A study over 4 years found that there was slower progression of T2 values in patients with a 10% decrease in body mass index and faster progression of T2 values in those with increased physical activity, as well as those with sedentary lifestyle.[10]

There were contradicting data on the correlation between severity of OA and T2 mapping. Dunn et al. reported that the higher the OA stage, the T2 values tended to increase as well,[15] while several others, such as a study by Koff et al., showed no definite difference in T2 value across OA stages.[16] In some chondral lesions, a heterogenous T2 pattern with the areas of low T2 value was observed rather than the areas of solely high T2.[1,17] The mechanism for the low T2 values in the chondral lesions is not well comprehended.

Although numerous investigators studied T2 mapping, their methodology was not consistent. In addition, healthy cartilage T2 values were not standardized.[18] Most of the studies used either a sagittal or coronal plane for cartilage mapping, focusing on limited area of subregions.[14,18,19] T2 mapping is the most researched and can be incorporated relatively easily on most clinical MRI systems. The pulse sequences and software required for generating T2 maps are now offered in commercial packages and do not require special coils.[9]

T1rho imaging

T1rho mapping is similar to T2 mapping except, after the magnetization is tipped into the transverse plane, it requires an additional radiofrequency pulse.[10] Similar to T2 mapping, there is no requirement for contrast administration, but it needs an MR scanner with the ability to generate a customized pulse sequence.[10] Damaged cartilage generally exhibits higher T1rho value.[20,21] In cartilage degeneration, depletion of proteoglycans is one of the earliest changes.[22,23] Decrease in proteoglycan content in cartilage correlates with alteration in T1rho values. Evidence shows that factors in addition to proteoglycan depletion contribute to the T1rho value, including orientation of collagen fiber and concentration of other macromolecules which are characteristic findings of the early stage of OA.[24] T1rho is higher in advanced OA in comparison with intermediate OA.[25]

Several studies suggest higher sensitivity of T1rho than T2 mapping in the detection of cartilage degeneration.[1,20,26,27] Regatte et al. compared the T1rho and T2 values obtained from surgical human specimens and concluded that T1rho has higher dynamic range than what can be used to detect smaller cartilage changes with a higher grade of accuracy. That study also showed that T1rho increase with OA grades was higher (30%–120%) than T2 (5%–50%).[28]

Although numerous studies show that T1rho is more sensitive for cartilage degeneration, measurement requires special pulse sequences, which lead to the use of high RF power and thus high specific absorption rate (SAR). Recent technical developments have since been developed to mitigate these risks.[29,30]

Delayed gadolinium-enhanced MRI of cartilage (dGEMRIC)

For dGEMRIC, intravenous contrast-medium administration is necessary for quantitative cartilage assessment. Normal cartilage contains negatively charged GAGs. After Gd-DTPA^{2-} injection in OA knee, negatively charged contrast agent tends to aggregate in degenerative cartilage where proteoglycan content is low (decreased negative charge), resulting in diminished T1 value compared with normal cartilage. Therefore, concentration of Gd-DTPA^{2-} contrast in normal cartilage with normal GAG will be generally low, while its concentration will be relatively high in damaged cartilage. Gd-DTPA^{2-} distribution in cartilage can be quantified from MR measurements of T1value to indirectly assess GAG content. which is known as dGEMRIC.[22,31,32]

Typically, the joint is moved for approximately 10 min following intravenous administration of gadolinium contrast, and images are acquired after 90-min delay. The time interval allows contrast diffusion and penetration into hyaline cartilage to reach equilibration. Different time delays may be used from joint to joint.[33]

Multiple studies validated that dGEMRIC is sensitive and specific for the quantification of GAG and thus OA. One study demonstrated that values in medial tibiofemoral compartments decrease with increase in radiographic Kellgrene-Lawrence grade.[34] Also, low T1 relaxation time in femoral cartilage after contrast administration (i.e. increase in cartilage signal on post-contrast T1-weighted images) was correlated with the development of osteophytes and the higher grade of joint space narrowing after a follow-up of 11 years.[35]

High sensitivity and specificity of dGEMRIC were validated in some studies making this method considered the gold standard. A disadvantage of dGEMRIC is the requirement for double-dose intravenous contrast injection. In addition, this technique is time consuming due to required exercise and time delay post-contrast injection.[22] Potential future introduction of this technique in clinical practice at 7 T will benefit from a reduction in scanning time, which can be obtained by omitting the pre-contrast T1 mapping acquisition.[36] Indeed, post-contrast T1 values were demonstrated sufficient to assess the cartilage health status in the hip at 7 T.

Sodium MRI

Proteoglycan is composed of a protein core, which is attached to many GAGs. The carboxyl and sulfate groups of GAGs are responsible for the negative fixed charge density (FCD). The FCD in order to achieve electrical neutrality attracts positive ions, such as sodium.[37] Sodium in cartilage is much higher than sodium in the adjacent synovial fluid or bone. Therefore, quantitative sodium MRI has been shown to be highly specific for the GAG content in cartilage. Sodium is relatively high in normal cartilage with abundant proteoglycan, while in damaged cartilage, there is proteoglycan, and therefore FCD and sodium concentration will be low.[10,38] Several studies validated the high sensitivity of sodium imaging.[37,39,40] There is also potential for post-operative cartilage repair assessment.[41]

Both the Larmor frequency and concentration of sodium are relatively lower than that of the proton. Sodium has also a short T2 relaxation time. These factors result in images with low resolution (2–4 mm isotropic), low SNR, and long acquisition time of around 15–30 min.[42] The low resolution result in observed partial volume affects from the surrounding synovial fluid and subchondral bone edema. Another challenge in the use of sodium imaging is that it requires the use of high magnetic field (e.g., 3 T and 7 T) with high magnetic field gradients and special RF coils.

On the bright side, a number of recently developed techniques can increase the spatial resolution and lessen the scan time.[43] Improvements in the sodium acquisition could be to further increase the spatial resolution, which can be done using dedicated sequences, such as, for instance, 3D cones, variable TEs gradient echo or density-adapted radial sequences, which could be carried out with uTE pulses.[44] Machine learning seems to be a potentially applicable technology for classifying OA patients and controls from sodium MRI data.[45] Advantages of sodium imaging are that sodium is a naturally occurring element and does not require contrast agent administration.

DWI and DTI

Evaluation with diffusion imaging is based on the ease of water molecules within the cartilage collagen matrix and proteoglycans. Since DWI can detect water motion in tissues, it can provide pertinent information in regard to tissue structure. Multiple gradient pulses are applied to incite magnetization in water molecules, but water gains a random amount of phase and cannot refocus, which results in loss of signal in tissues undergoing diffusion.[17,22] In normal healthy cartilage, water movement is restricted by the rest of cartilage components, leading to low apparent diffusion coefficient (ADC) signal. On the other hand, cartilage degeneration and disruption of the normal structure enhance water mobility and increase ADC cartilage signal. These changes in ADC values can be mapped.[46]

In vivo DWI cartilage mapping remains challenging due to short T2 of cartilage. Also, DWI is sensitive to motion artifacts and navigator motion correction is required. These factors make it difficult to achieve the resolution needed for cartilage assessment.[17,47–49] Nevertheless, advancing in imaging techniques shows that DWI seems to have a potential in the evaluation of cartilage degeneration, as well as in monitoring post-repair changes.[47,50,51]

In addition to DWI, DTI can also be applied to cartilage imaging, evaluating directions of water within the extracellular matrix. In the normal cartilage, the microarchitecture leads to anisotropic diffusion of water. Therefore, changes in anisotropy are likely caused by changes in the microarchitecture of cartilage.[52] The concept of DTI is related to the known collagen fiber orientation in multiple layers. Work by Meder et al. on the samples of bovine knee joints suggested that orientation of the maximum diffusion eigenvectors is related to collagen fiber orientation and arrangement.[53] Recent reports have shown that DTI has the possibilities as a marker for joint degradation and can shed light on the integrity of the articular cartilage with good reproducibility.[52–58]

As with diffusion and ADC studies, it is challenging to use DTI as a marker in the clinical setting due to difficulty in balancing SNR, resolution, and acceptable scan time.[55]

uTE

Conventional spin echo sequences usually use TE of around 10 msec. In these sequences, low T2 structures, such as ligaments, tendons, menisci, deep calcified layers of cartilage and the cortex of the bones, will demonstrate low signal, and their internal structures are undetected. Much shorter TEs (uTE) are now achievable with gradient echo pulse sequences in the range of 0.05–0.20 msec by using half RF excitations with radial mapping from the center of k-space. The use of uTE technique enables the detection of signals from those structures.[59,60]

The osteochondral junction consists mainly of the subchondral bone and calcified layer of the cartilage (CC). The junction transports solute between the cartilage and the vessels, which has been implicated in the pathogenesis of OA. The calcified cartilage is of importance in chondral repair processes. It was reported that CC removal would lead to a better surgical outcome.[22,60–62] The uTE imaging can better demonstrate the zonal architecture of cartilage and help delineate the deepest layers, including CC.

In a study by Bae et al., the subtracted images of the human patella with two complementary techniques demonstrated linear high signal intensity near the osteochondral junction. They have concluded that the high signal was contributed by the deepest layer of the uncalcified cartilage and the calcified cartilage with no significant contribution from the subchondral bone.[60]

As with other quantitative methods, there are certain difficulties observed. These challenges in uTE imaging include error in the radial k-space trajectories, off-resonance, and distortion of the slice profile. However, gradient calibration, off-resonance correction, and efficient fat suppression may help improve the outcome.

gagCEST

The gagCEST is a relatively newer compositional MRI technique based on the constant transfer of labile protons between solutes and water. Exchange saturation transfer is based on the fact that water in extracellular matrix is either free or bound to macromolecules. An off-resonance RF pulse can be used to saturate water associated with macromolecules. The saturation is then exchanged with the free water leading to signal loss. gagCEST imaging uses RF pulses applied at frequencies specific to exchangeable protons residing in GAG, thereby proposing a method for quantitative cartilage imaging. In the areas of GAG loss, lower gagCEST values are demonstrated.

Seven T MRI improves the gagCEST performance for the increased SNR, as well as for the more selective saturation between hydroxyl GAG and water protons due to the increased gap in resonance frequencies.[36] In a study utilizing 7 T MR, there was a high correlation between gagCEST and sodium imaging in post-cartilage repair assessment.[63] Due to limited frequency difference between hydroxyl protons and water, better spectral separation at 7 T is preferred over 3 T. Although the gagCEST still has limits, a study using 3 T MR found gagCEST comparable to T2 mapping and dGEMRIC in detecting normal and damaged cartilage.[64] There may be a potential for gagCEST to play an increasing role in research and clinical settings.

Quantitative Cartilage Analysis – Layer (Depth)-Dependent Approach

Cartilage zones (layers)

Cartilage consists of four zones (layers) from the articular surface to the subchondral bone plate: superficial (tangential) zone, transitional zone, radial or deep zone, and calcified cartilage zone. The superficial zone is thin and protects deeper layers from shear stresses.[65] The transitional zone provides an anatomic and functional bridge between the

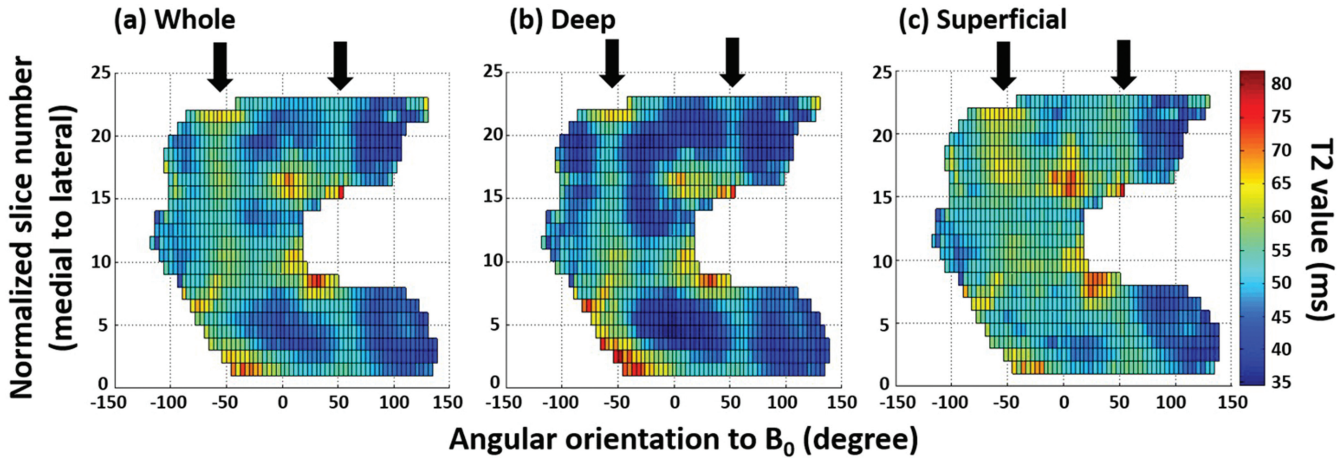

Fig. 1 T2 profiles on 2D surface map of (**a**) the whole layer, (**b**) the deep layer, and (**c**) the superficial layer of the entire femoral cartilage. Arrows indicate ± 54.7° (the magic angle). (Reprinted with permission from #6).

superficial and deep zones. It contains abundant proteoglycans and thicker type II collagen in an organized oblique direction. The deep zone is responsible for providing the greatest resistance to compressive forces. It consists of collagen fibrils perpendicular to the articular surface and crosses the tidemark. The deep layer contains the highest concentration of proteoglycans and the lowest water concentration. The calcified layer plays an integral role in securing the cartilage to bone by anchoring the collagen fibrils of the deep zone to subchondral bone.

Quantitative analysis of layer (depth)-dependent approach

Cartilage degeneration affects the zonal variation in T2 relaxation times. Normal articular hyaline cartilage illustrates a predictable zonal variation in T2 relaxation times with increasing T2 values from the subchondral bone to the articular surface.[6,66] In the deep zone of normal hyaline cartilage, the collagen fibers run perpendicular to the cortical surface. Therefore, the magic angle effect was more apparent in the deep layer compared with the superficial layer within both the medial and lateral condyles (Fig. 1).[6] Toward the articular surface, the fibers have a more oblique or random orientation that causes a different mobility for water protons in this partly anisotropic tissue.[67] Because of spatial resolution limitations, in many zonal variation studies, the cartilage ROIs were divided into two equal-sized deep and superficial layers (Fig. 2). Apprich et al. reported that the T2 relaxation times increase with increasing cartilage defect grade, especially T2 values of the superficial layer. However, the zonal variation is even present in higher grades of cartilage degeneration.[66] Mamisch et al. evaluated T2 values in the superficial and deep layers on a high-resolution knee MRI at different time points after matrix-associated autologous chondrocyte transplantation (MACT).[68] The results were that, for the zonal T2 values, native control cartilage of the early and late unloading measurements showed significantly higher T2 values in the superficial zone, but not in the deep zone. In contrast, the zonal evaluation of the cartilage repair tissue showed significantly higher T2 relaxation times for the early and late unloading for both cartilage layers. This result suggested that T2 relaxation times can be used to assess the early and late unloading values of articular cartilage in a clinical setting and that the time point of the quantitative T2 measurement affects the differentiation between native and abnormal articular cartilage.

Regarding zonal variation of T1rho relaxation times, T1rho values were higher in the superficial layer than in the deep layer in most locations in the medial and lateral condyles, including the weight-bearing portion (Fig. 3).[69] In a previous study, T1rho values were higher in the non-weight-bearing portion than in the weight-bearing portion over the medial and lateral condyles.[69] This finding is more significant in the deep layer. In other words, proteoglycan content was greater and T1rho values were lower in the weight-bearing portion, especially in the deep layer. Proteoglycans resist compression and generate swelling pressure due to their affinity for water. The deep zone consists of large-diameter collagen fibrils oriented perpendicular to the articular surface. This layer contains the highest proteoglycan, lowest water concentration, and highest compressive modulus.[3] More resistance to various forces in knee activity is required in the weight-bearing portion. Therefore, it makes sense that cartilage in the weight-bearing portion needs more proteoglycan, which results in lower T1rho values in this region.

Quantitative Cartilage Analysis – Regional (Angle)-Dependent Approach

Signal variations of normal knee cartilage

Articular cartilage signal of the knee joint is not uniform in conventional MRI. In addition to signal variations in each

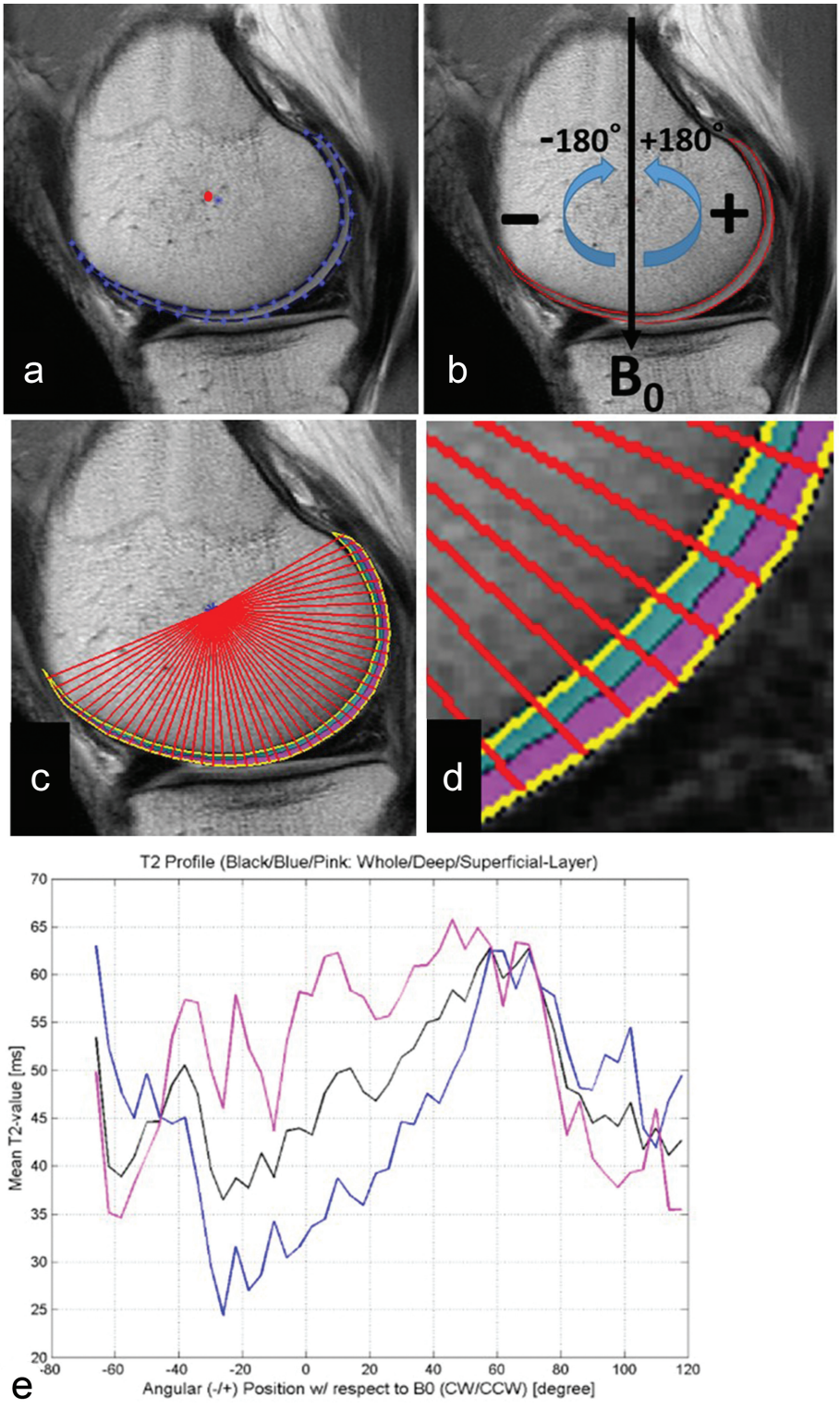

Fig. 2 Articular segmentation with angle- or layer-dependent approach. (**a**) After manual cartilage extraction, the central point of the cartilage (red dot) was automatically approximated. (**b**) Static magnetic field (B0) was defined as 0 degrees, with negative and positive angles located anterior and posterior to the central point. (**c**) Radial lines from a central point divided cartilage into 4-degree segments. (**d**) Segmentation of cartilage into deep (0%–50%) and superficial layers (51%–100%) of relative thickness. (**e**) T2 profiles were generated for whole thickness, deep, and superficial layers of cartilage. (Reprinted with permission from #6).

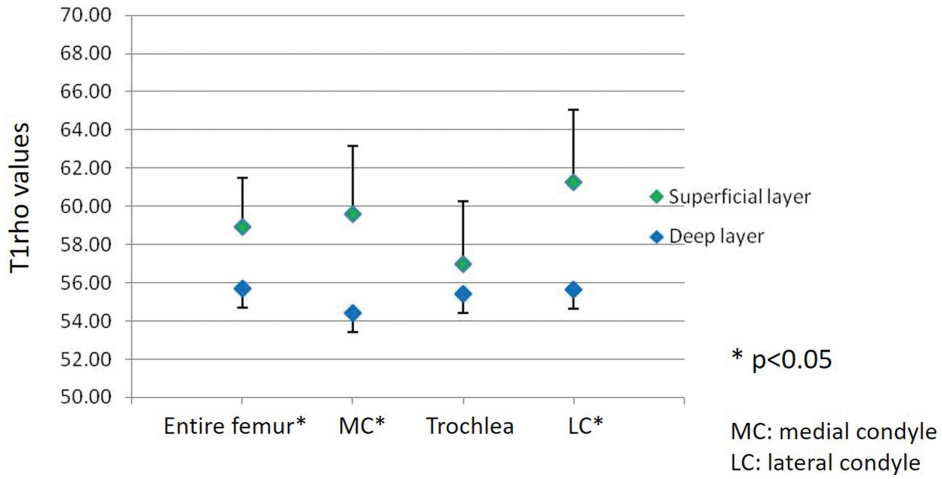

Fig. 3 Difference in average T1rho values between the superficial and deep layers at the medial condyle, lateral condyle, trochlea, and the entire femoral cartilage. Average T1rho values in the superficial layer of the femoral articular cartilage are higher than in the deep layer over the entire femur, medial condyle, and lateral condyle, with a statistically significant difference ($P < 0.05$). (Reprinted with permission from #67).

cartilage layer in the depth direction, there are variations of cartilage signal intensities in various areas within the knee with fat-suppressed fast spin echo (FSE) and 3D spoiled gradient-recalled echo sequence (SPGR) images in conventional MRI.[70] For example, decreased signal intensity in the distal part of the trochlear cartilage was seen on images obtained with all sequences in all volunteers and patients with OA. The cause of the very low signal intensity in this region is not clear, but it is presumably related to the anisotropic arrangement of collagen fibers. Another normal appearance on fat-suppressed SPGR MR images was a linear area of low signal intensity in the center of the cartilage that was probably caused by truncation artifact, which was present in the patellofemoral compartment in 96% of the patients and in the posterior region of the femoral condyles in 86% of the patients. Approximately one-fourth patients showed linear high signal intensity truncation artifact within intermediate or low signal cartilage with FSE proton density (PD) or T2 sequences in the same location.

Magic angle effects

The magic angle is an MRI artifact, which occurs on sequences with a short TE and causes increased signal intensity. The magic angle effect is commonly seen and is important in the clinical MRI of certain tissues (especially tendons, cartilage, and peripheral nerves) that are highly structured and are oriented obliquely to the main magnetic field at 54.74° from the main magnetic field (B0). The magic angle effect causes laminar appearance of articular cartilage. The direct cause is the T2 relaxation anisotropy in the tissue, which is closely linked to the structure of the collagen fibers, their orientation in the magnetic field, and the water–proteoglycan interaction. This amplifies the prevailing orientation of the collagen fiber network.[71]

Quantitative analysis of angular dependent approach

Kaneko et al. analyzed the entire femoral cartilage at the knee joint by angular segmentations in steps of 4-degrees over the length of the segmented cartilage (Fig. 2).[6] Magic angle effect on T2 mapping was clearly observed in the both medial and lateral femoral condyles, especially within the whole and deep layers (Fig. 1). However, there were no significant differences between the magic angle and other angles within the superficial layer of the medial condyle. The authors suggested that this might be due to the small sample size. Another plausible explanation would be that structural anisotropy of the collagen fibers decreases the magic angle effect on the superficial layer.[6] Nozaki et al. reported normalized T1rho profiles of the entire femoral cartilage in healthy subjects using similar manner in regard to angular segmentation as above.[69] Although T1rho profiles are not homogeneous over the entire femur and there is angle-dependent variation in T1rho, there is no influence of magic angle effect on T1rho profiles. In general, T2 and T1rho values increase in degenerative cartilage. However, in a previous study of early knee OA, the median values of T2 and T1rho around the magic angle for early OA patients actually tended to show lower values in both the deep and superficial layers compared with those of the controls.[1] This is due to the fact that normal cartilage T2 and T1rho around the magic angle are relatively increased compared to those of early degeneration. Another example of reginal or angle dependent variations involves the most distal trochlea. Meanwhile, T2 and T1rho are decreased in healthy volunteers, especially in the deep layer as fat-suppressed proton density-weighted imaging (FS PDWI) normally demonstrates low signal intensity.[70] Therefore, increased T2 and T1rho values around the most distal trochlea should be considered abnormal. These examples highlight the fact that, in order to accurately detect early cartilage

degeneration using T2 and T1rho values, it is necessary to know the fact that cartilage T2 and T1rho have reginal- or angle-dependent variations and to compare values between potential lesions and expected regional specific normal cartilage values.

Cluster analysis

Cluster analysis has been used to identify focal regions of elevated or decreased quantitative metrics on individual projection maps of averaged pixel data within angular bins. Monu et al. classified clusters as either increased or decreased by setting two thresholds: intensity and size. For both cartilage T2 and T1rho relaxation times, thresholds for increased and decreased clusters were set at +2 mean standard deviation of the healthy groups' difference map.[72] A cluster was defined as a contiguous set of pixels above or below these thresholds. Using cluster analysis technique, they have quantified cartilage lesion coverage and demonstrated that the anterior cruciate ligament (ACL)-injured group had greater areas of elevated T2 and T1rho relaxation times as compared to healthy volunteers. The cluster analysis uses the subtracting projection maps from the healthy population to set the intensity threshold and cluster size across populations. It is essential to account for the magic angle effect that could lead to incorrect detection of the areas of elevated T2 and to a lesser extent T1rho relaxation times. Also, selecting appropriate cluster size allows for characterizing focal lesions by mitigating the effects of noise, such as single voxel changes while still capturing focal lesions.[72] T2 cluster analysis has been used for bilateral femoral cartilage T2 asymmetry analysis of the detection of early OA,[73] early changes in ACL-reconstructed knee,[74] and acute exercise in knee OA.[75]

Quantitative MR Evaluation after Cartilage Repair

Quantitative MRI is useful to evaluate repaired cartilage as a non-invasive imaging modality without arthroscopy or biopsy. T1rho mapping, T2 mapping, dGEMRIC, and DWI are applicable to most clinical MR scanners. Currently, there are several cartilage repair techniques, including microfracture (Mfx), osteochondral autograft transplantations (OAT), and autologous chondrocyte implantation (ACI) or matrix-associated ACI (MACI). We should keep in mind that different cartilage repair techniques are known to result in repair tissues with different histological compositions that vary during maturation.[9] One of the advantages of quantitative cartilage MRI is to demonstrate structural difference between different cartilage repair techniques or between repaired cartilage and surround normal cartilage quantitatively and noninvasively. For example, after Mfx, tissue has been mostly reported as fibrous cartilage, which shows lower T2 relaxation times than normal hyaline cartilage. After ACI or MACI, tissue has been characterized as hyaline-like. Kurkijärvi et al. showed that T2 values for ACI repair tissue were higher and more heterogeneous than T2 of normal control cartilage about 1 year after surgery with a lack of zonal organization.[76] T1rho was found to be elevated in cartilage repair tissue after OAT and Mfx as compared to normal cartilage up to 1 year after surgery.[77] Watanabe et al. reported that dGEMRIC measurements correlated with the GAG content of the ACI grafts.[78]

However, there are several limitations of quantitative MR evaluation after cartilage repair. First, Shimomura et al. reported that there were no correlations detected between histological scores and T2 values for each repair cartilage zone.[79] This result suggests that T2 mapping is limited to demonstrate accurate zonal variations after repair. Second, the results from previous studies are sometimes divergent because of different cartilage repair techniques and different maturation process, as well as different quantitative MR imaging techniques, including different imaging protocols, different coils, different analysis methods, and different patient cohorts. Third, clinical correlations are limited, and clinical importance including prediction of procedure outcome needs to be demonstrated in larger cross-sectional and longitudinal cohort studies.[77] Finally, manual segmentation is required in many cases, which is limited by inter- and intraobserver reliability errors. Deep learning may solve this segmentation issue in the future.

Quantitative Cartilage MRI Combined with New Techniques

Main challenges of quantitative cartilage MRI are long acquisition times and low spatial resolution. In other words, new techniques with shorter acquisition time and higher spatial resolution are desired in the present and future. Compressed sensing (CS) is a novel concept for reconstructing images from highly undersampled data. CS has the potential to greatly shorten scanning times and has many different applications, including quantitative cartilage map sequences.[29] CS theory affirms that certain signals and images can be recovered from highly compressed k-space data with an appropriate reconstruction algorithm. To make this possible, CS should meet three requirements: sparsity, incoherence of a sampling trajectory, and nonlinear reconstruction. Efficient data acquisition using CS is extremely important for compositional mapping of the musculoskeletal system, in general, and knee cartilage mapping techniques, in particular.[80] High-resolution quantitative information about tissue biochemical composition could be obtained in just a few minutes using CS MRI (Fig. 4). The combination of parallel imaging and CS are especially useful. Both are fast imaging techniques that could potentially accelerate the acquisition speed of cartilage quantitative imaging by means of k-space undersampling below the Nyquist rate.[81]

Regarding cartilage T2 mapping using CS, Huang et al. reported that CS T2 mapping data were acquired in only 2 min and 12 s compared with the 17 min and 8 s acquisition

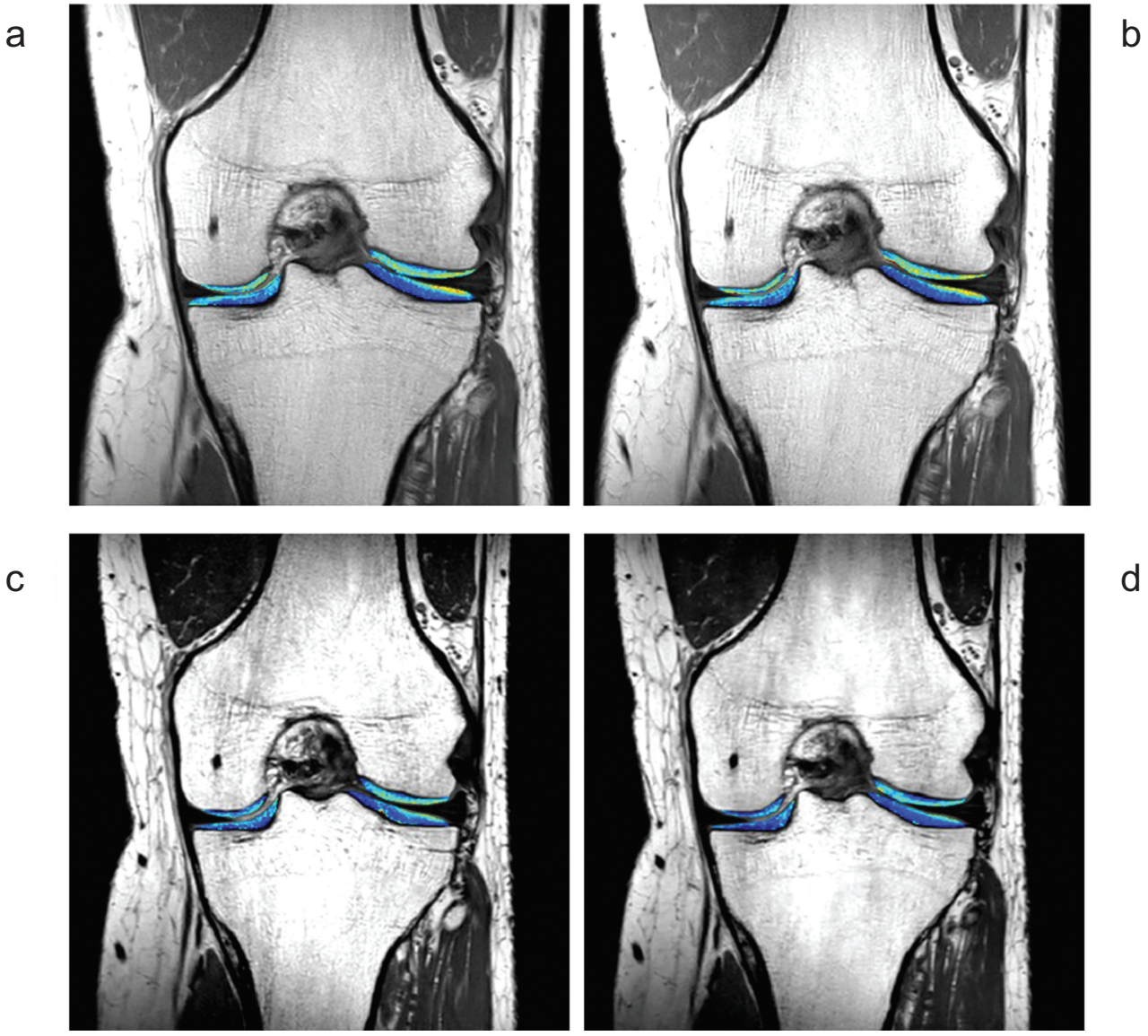

Fig. 4 2D and 3D knee cartilage T2 mapping using SENSE or CS. (**a**) 2D T2 mapping with SENSE (factor = 2, 7 min 5 sec), (**b**) 2D T2 mapping with CS (factor = 3, 4 min 44 sec), (**c**) 3D T2 mapping with SENSE (factor = 4, 11 min 28 sec), and (**d**) 3D T2 mapping with CS (factor = 6, 8 min 2 sec). (Courtesy of Dr. Atsuya Watanabe and Mr. Takayuki Sakai at Eastern Chiba Medical Center, Japan). CS, compressed singing; SENSE, sensitivity encoding.

needed for the gold standard T2 map reconstructed from eight TE images with 256 k-space radial lines each.[82] Wang et al, reported that, for macroscopic MRI, where the resolution mimics the clinical MRI of human cartilage, the quantitative T2 mapping at accelerating factors up to 4 times showed negligible variations.[83] Therefore, clinical MRI can benefit from the use of CS in image acquisition without losing significant accuracy in the quantification of T2 maps in osteoarthritic cartilage.

Zhou et al. combine an advanced CS-based dynamic imaging technique, k-t locally adaptive iterative support detection (LAISD) and an advanced parallel imaging technique (joint image reconstruction and sensitivity estimation in SENSE [JSENSE]) to achieve maximum acceleration of cartilage T1rho imaging.[81] T1rho maps obtained from accelerated scans (acceleration factors of 3 and 3.5) showed results comparable to conventional full scans without sacrificing accuracy (T1rho errors in all compartments below 1%). They concluded that CS will greatly facilitate the clinical translation of quantitative cartilage MRI. 3D sequences usually come at the cost of a significant increase in scan time. Zibetti et al. reported that accelerating 3D T1ρ mapping of cartilage with CS using specific sparsifying transforms is feasible up to accelerations factors of 10 with T1rho errors below 6.5%.[80]

The preliminary study by Madelin et al. showed that CS can be applied to sodium MRI of cartilage at 7 T in order to decrease the acquisition time by a factor of 2 without losing accuracy in tissue sodium concentration over different ROIs in the cartilage for detecting early signs of OA.[84] A further improvement, upon acquisition of multichannel double-tuned (1H + 23Na) RF knee coils at 3 T and 7 T, would be to apply CS sodium MRI in combination with parallel imaging to further reduce the imaging time by another factor 2 or 3.[84]

The performance of CS is limited in cases where the fully sampled image already has low SNR. This makes the application of CS to DWI challenging since diffusion-weighted images inherently have lower SNR. Knoll et al. introduce a new image reconstruction technique for DTI, which combines the concepts of parallel imaging, model-based reconstruction, and CS.[85] They concluded that this may enable an essential reduction in the acquisition time in radial spin echo DTI without degrading parameter quantification and/or SNR.[85]

MR fingerprinting (MRF) is a new approach to quantitative MRI that allows simultaneous measurement of multiple tissue properties in a single time-efficient acquisition.[86] This technique can estimate multiple MR parameters simultaneously (e.g., T1 and T2) using dynamic signal patterns.[87] Sharafi et al. demonstrated the feasibility of an MRF sequence that can simultaneously measure the T1, T2, and T1ρ maps in a single scan.[87] Their *in vivo* results showed that it could distinguish the mild OA patients from the healthy controls and has the potential to be used for the quantitative assessment of the cartilage for the early detection of OA.

Conflicts of Interest

The authors declare that there is no conflict of interest related to this work.

References

1. Kaneko Y, Nozaki T, Yu H, et al. Assessing patterns of T2/T1rho change in grade 1 cartilage lesions of the distal femur using an angle/layer dependent approach. Clin Imaging 2018; 50:201–207.
2. Fujinaga Y, Yoshioka H, Sakai T, et al. Quantitative measurement of femoral condyle cartilage in the knee by MRI: validation study by multireaders. J Magn Reson Imaging 2014; 39:972–977.
3. Pearle AD, Warren RF, Rodeo SA. Basic science of articular cartilage and osteoarthritis. Clin Sports Med 2005; 24:1–12.
4. Bruno F, Arrigoni F, Palumbo P, et al. New advances in MRI diagnosis of degenerative osteoarthropathy of the peripheral joints. Radiol Med 2019; 124:1121–1127.
5. Wang N, Badar F, Xia Y. Experimental influences in the accurate measurement of cartilage thickness in MRI. Cartilage 2019; 10:278–287.
6. Kaneko Y, Nozaki T, Yu H, et al. Normal T2 map profile of the entire femoral cartilage using an angle/layer-dependent approach. J Magn Reson Imaging 2015; 42:1507–1516.
7. Goodwin DW, Zhu H, Dunn JF. *In vitro* MR imaging of hyaline cartilage: correlation with scanning electron microscopy. AJR Am J Roentgenol 2000; 174:405–409.
8. Nieminen MT, Rieppo J, Töyräs J, et al. T2 relaxation reveals spatial collagen architecture in articular cartilage: a comparative quantitative MRI and polarized light microscopic study. Magn Reson Med 2001; 46:487–493.
9. Crema MD, Roemer FW, Marra MD, et al. Articular cartilage in the knee: current MR imaging techniques and applications in clinical practice and research. Radiographics 2011; 31:37–61.
10. Guermazi A, Alizai H, Crema MD, et al. Compositional MRI techniques for evaluation of cartilage degeneration in osteoarthritis. Osteoarthritis Cartilage 2015; 23:1639–1653.
11. Baum T, Joseph GB, Karampinos DC, et al. Cartilage and meniscal T2 relaxation time as non-invasive biomarker for knee osteoarthritis and cartilage repair procedures. Osteoarthritis Cartilage 2013; 21:1474–1484.
12. Zhong H, Miller DJ, Urish KL. T2 map signal variation predicts symptomatic osteoarthritis progression: data from the Osteoarthritis Initiative. Skeletal Radiol 2016; 45:909–913.
13. Wu Y, Yang R, Jia S, et al. Computer-aided diagnosis of early knee osteoarthritis based on MRI T2 mapping. Biomed Mater Eng 2014; 24:3379–3388.
14. Mosher TJ, Smith H, Dardzinski BJ, et al. MR imaging and T2 mapping of femoral cartilage: *in vivo* determination of the magic angle effect. AJR Am J Roentgenol 2001; 177:665–669.
15. Dunn TC, Lu Y, Jin H, et al. T2 relaxation time of cartilage at MR imaging: comparison with severity of knee osteoarthritis. Radiology 2004; 232:592–598.
16. Koff MF, Amrami KK, Kaufman KR. Clinical evaluation of T2 values of patellar cartilage in patients with osteoarthritis. Osteoarthritis Cartilage 2007; 15:198–204.
17. Gold GE, Burstein D, Dardzinski B, et al. MRI of articular cartilage in OA: novel pulse sequences and compositional/functional markers. Osteoarthritis Cartilage 2006; 14 (Suppl A):A76–86.
18. Surowiec RK, Lucas EP, Fitzcharles EK, et al. T2 values of articular cartilage in clinically relevant subregions of the asymptomatic knee. Knee Surg Sports Traumatol Arthrosc 2014; 22:1404–1414.
19. Smith HE, Mosher TJ, Dardzinski BJ, et al. Spatial variation in cartilage T2 of the knee. J Magn Reson Imaging 2001; 14:50–55.
20. Stahl R, Luke A, Li X, et al. T1rho, T2 and focal knee cartilage abnormalities in physically active and sedentary healthy subjects versus early OA patients—a 3.0-Tesla MRI study. Eur Radiol 2009; 19:132–143.
21. Regatte RR, Akella SV, Lonner JH, et al. T1rho relaxation mapping in human osteoarthritis (OA) cartilage: comparison of T1rho with T2. J Magn Reson Imaging 2006; 23:547–553.
22. Choi JA, Gold GE. MR imaging of articular cartilage physiology. Magn Reson Imaging Clin N Am 2011; 19:249–282.
23. Akella SV, Reddy Regatte R, Gougoutas AJ, et al. Proteoglycan-induced changes in T1ρ-relaxation of articular cartilage at 4T. Magnet Reson Med 2001; 46:419–423.

24. Mlynárik V, Trattnig S, Huber M, et al. The role of relaxation times in monitoring proteoglycan depletion in articular cartilage. J Magn Reson Imaging 1999; 10:497–502.
25. Koskinen SK, Ylä-Outinen H, Aho HJ, et al. Magnetization transfer and spin lock MR imaging of patellar cartilage degeneration at 0.1 T. Acta Radiol 1997; 38:1071–1075.
26. Wang L, Regatte RR. Quantitative mapping of human cartilage at 3.0T: parallel changes in T_2, $T_1\rho$, and dGEMRIC. Acad Radiol 2014; 21:463–471.
27. Thuillier DU, Souza RB, Wu S, et al. T1ρ imaging demonstrates early changes in the lateral patella in patients with patellofemoral pain and maltracking. Am J Sports Med 2013; 41:1813–1818.
28. Regatte RR, Akella SV, Reddy R. Depth-dependent proton magnetization transfer in articular cartilage. J Magn Reson Imaging 2005; 22:318–323.
29. Chang AL, Yu HJ, von Borstel D, et al. Advanced Imaging Techniques of the Wrist. AJR Am J Roentgenol 2017; 209:497–510.
30. Wheaton AJ, Borthakur A, Corbo M, et al. Method for reduced SAR T1ρ-weighted MRI. Magnet Reson Med 2004; 51:1096–1102.
31. Gray ML, Burstein D. Molecular (and functional) imaging of articular cartilage. J Musculoskelet Neuronal Interact 2004; 4:365–368.
32. Gray ML, Burstein D, Xia Y. Biochemical (and functional) imaging of articular cartilage. Semin Musculoskelet Radiol 2001; 5:329–343.
33. Burstein D, Velyvis J, Scott KT, et al. Protocol issues for delayed Gd(DTPA)(2-)-enhanced MRI (dGEMRIC) for clinical evaluation of articular cartilage. Magn Reson Med 2001;45:36–41.
34. Crema MD, Hunter DJ, Burstein D, et al. Association of changes in delayed gadolinium-enhanced MRI of cartilage (dGEMRIC) with changes in cartilage thickness in the medial tibiofemoral compartment of the knee: a 2 year follow-up study using 3.0 T MRI. Ann Rheum Dis 2014; 73:1935–1941.
35. Owman H, Ericsson YB, Englund M, et al. Association between delayed gadolinium-enhanced MRI of cartilage (dGEMRIC) and joint space narrowing and osteophytes: a cohort study in patients with partial meniscectomy with 11 yrs of follow-up. Osteoarthritis Cartilage 2014; 22:1537–1541.
36. Aringhieri G, Zampa V, Tosetti M. Musculoskeletal MRI at 7 T: do we need more or is it more than enough?. Eur Radiol Exp 2020; 4:48.
37. Wheaton AJ, Borthakur A, Shapiro EM, et al. Proteoglycan loss in human knee cartilage: quantitation with sodium MR imaging—feasibility study. Radiology 2004; 231:900–905.
38. Burstein D, Gray M, Mosher T, et al. Measures of molecular composition and structure in osteoarthritis. Radiol Clin North Am 2009; 47:675–686.
39. Shapiro EM, Borthakur A, Gougoutas A, et al. 23Na MRI accurately measures fixed charge density in articular cartilage. Magn Reson Med 2002; 47:284–291.
40. Borthakur A, Shapiro EM, Akella SV, et al. Quantifying sodium in the human wrist *in vivo* by using MR imaging. Radiology 2002; 224:598–602.
41. Trattnig S, Welsch GH, Juras V, et al. 23Na MR imaging at 7 T after knee matrix-associated autologous chondrocyte transplantation preliminary results. Radiology 2010; 257:175–184.
42. Madelin G, Babb JS, Xia D, et al. Reproducibility and repeatability of quantitative sodium magnetic resonance imaging *in vivo* in articular cartilage at 3 T and 7 T. Magn Reson Med 2012; 68:841–849.
43. Wang L, Wu Y, Chang G, et al. Rapid isotropic 3D-sodium MRI of the knee joint *in vivo* at 7T. J Magn Reson Imaging 2009; 30:606–614.
44. Brinkhof S, Froeling M, Janssen RPA, et al. Can sodium MRI be used as a method for mapping of cartilage stiffness? MAGMA 2021; 34:327–336.
45. Madelin G, Poidevin F, Makrymallis A, et al. Classification of sodium MRI data of cartilage using machine learning. Magn Reson Med 2015; 74:1435–1448.
46. Burstein D, Gray ML, Hartman AL, et al. Diffusion of small solutes in cartilage as measured by nuclear magnetic resonance (NMR) spectroscopy and imaging. J Orthop Res 1993; 11:465–478.
47. Miller KL, Hargreaves BA, Gold GE, et al. Steady-state diffusion-weighted imaging of *in vivo* knee cartilage. Magn Reson Med 2004; 51:394–398.
48. Anderson AW, Gore JC. Analysis and correction of motion artifacts in diffusion weighted imaging. Magn Reson Med 1994; 32:379–387.
49. Ordidge RJ, Helpern JA, Qing ZX, et al. Correction of motional artifacts in diffusion-weighted MR images using navigator echoes. Magn Reson Imaging 1994; 12:455–460.
50. Friedrich KM, Mamisch TC, Plank C, et al. Diffusion-weighted imaging for the follow-up of patients after matrix-associated autologous chondrocyte transplantation. Eur J Radiol 2010; 73:622–628.
51. Mamisch TC, Menzel MI, Welsch GH, et al. Steady-state diffusion imaging for MR in-vivo evaluation of reparative cartilage after matrix-associated autologous chondrocyte transplantation at 3 tesla—preliminary results. Eur J Radiol 2008; 65:72–79.
52. Raya JG, Melkus G, Adam-Neumair S, et al. Diffusion-tensor imaging of human articular cartilage specimens with early signs of cartilage damage. Radiology 2013; 266:831–841.
53. Meder R, de Visser SK, Bowden JC, et al. Diffusion tensor imaging of articular cartilage as a measure of tissue microstructure. Osteoarthritis Cartilage 2006; 14:875–881.
54. Filidoro L, Dietrich O, Weber J, et al. High-resolution diffusion tensor imaging of human patellar cartilage: feasibility and preliminary findings. Magn Reson Med 2005; 53:993–998.
55. Deng X, Farley M, Nieminen MT, et al. Diffusion tensor imaging of native and degenerated human articular cartilage. Magn Reson Imaging 2007; 25:168–171.
56. Azuma T, Nakai R, Takizawa O, et al. *In vivo* structural analysis of articular cartilage using diffusion tensor magnetic resonance imaging. Magn Reson Imaging 2009; 27:1242–1248.
57. Raya JG, Horng A, Dietrich O, et al. Articular cartilage: *in vivo* diffusion-tensor imaging. Radiology 2012; 262:550–559.
58. Raya JG, Melkus G, Adam-Neumair S, et al. Change of diffusion tensor imaging parameters in articular cartilage with

progressive proteoglycan extraction. Invest Radiol 2011; 46:401–409.
59. Robson MD, Gatehouse PD, Bydder M, et al. Magnetic resonance: an introduction to ultrashort TE (UTE) imaging. J Comput Assist Tomogr 2003; 27:825–846.
60. Bae WC, Dwek JR, Znamirowski R, et al. Ultrashort echo time MR imaging of osteochondral junction of the knee at 3 T: identification of anatomic structures contributing to signal intensity. Radiology 2010; 254:837–845.
61. Lyons TJ, McClure SF, Stoddart RW, et al. The normal human chondro-osseous junctional region: evidence for contact of uncalcified cartilage with subchondral bone and marrow spaces. BMC Musculoskelet Disord 2006; 7:52.
62. Hwang J, Bae WC, Shieu W, et al. Increased hydraulic conductance of human articular cartilage and subchondral bone plate with progression of osteoarthritis. Arthritis Rheum 2008; 58:3831–3842.
63. Schmitt B, Zbýn S, Stelzeneder D, et al. Cartilage quality assessment by using glycosaminoglycan chemical exchange saturation transfer and (23)Na MR imaging at 7 T. Radiology 2011; 260:257–264.
64. Rehnitz C, Kupfer J, Streich NA, et al. Comparison of biochemical cartilage imaging techniques at 3 T MRI. Osteoarthritis Cartilage 2014; 22:1732–1742.
65. Sophia Fox AJ, Bedi A, Rodeo SA. The basic science of articular cartilage: structure, composition, and function. Sports Health 2009; 1:461–468.
66. Apprich S, Welsch GH, Mamisch TC, et al. Detection of degenerative cartilage disease: comparison of high-resolution morphological MR and quantitative T2 mapping at 3.0 Tesla. Osteoarthritis Cartilage 2010; 18:1211–1217.
67. Mosher TJ, Dardzinski BJ. Cartilage MRI T2 relaxation time mapping: overview and applications. Semin Musculoskelet Radiol 2004; 8:355–368.
68. Mamisch TC, Trattnig S, Quirbach S, et al. Quantitative T2 mapping of knee cartilage: differentiation of healthy control cartilage and cartilage repair tissue in the knee with unloading—initial results. Radiology 2010; 254:818–826.
69. Nozaki T, Kaneko Y, Yu HJ, et al. T1rho mapping of entire femoral cartilage using depth- and angle-dependent analysis. Eur Radiol 2016; 26:1952–1962.
70. Yoshioka H, Stevens K, Genovese M, et al. Articular cartilage of knee: normal patterns at MR imaging that mimic disease in healthy subjects and patients with osteoarthritis. Radiology 2004; 231:31–38.
71. Xia Y. Magic-angle effect in magnetic resonance imaging of articular cartilage: a review. Invest Radiol 2000; 35:602–621.
72. Monu UD, Jordan CD, Samuelson BL, et al. Cluster analysis of quantitative MRI T2 and T1ρ relaxation times of cartilage identifies differences between healthy and ACL-injured individuals at 3T. Osteoarthritis Cartilage 2017; 25:513–520.
73. Black MS, Young KA, Chaudhari AS, et al. Bilateral femoral cartilage T2 asymmetry analysis for the detection of early osteoarthritic degeneration. Proceedings of the 2020 ISMRM & SMRT Virtual Conference & Exhibition, Online, 2020; 353.
74. Black MS, Young KA, Chaudhari AS, et al. Detecting early changes in ACL-reconstructed knees: cluster analysis of T2 relaxation times from 3 months to 18 months post-surgery. Proceedings of the 2020 ISMRM & SMRT Virtual Conference & Exhibition, Online, 2020; 2738.
75. Watkins L, Mazzoli V, Black M, et al. Cluster analysis of T2 changes is related to acute exercise in individuals with knee osteoarthritis. Proceedings of the 2020 ISMRM & SMRT Virtual Conference & Exhibition, Online, 2020; 2754.
76. Kurkijärvi JE, Mattila L, Ojala RO, et al. Evaluation of cartilage repair in the distal femur after autologous chondrocyte transplantation using T2 relaxation time and dGEMRIC. Osteoarthritis Cartilage 2007; 15:372–378.
77. Jungmann PM, Baum T, Bauer JS, et al. Cartilage repair surgery: outcome evaluation by using noninvasive cartilage biomarkers based on quantitative MRI techniques? Biomed Res Int 2014; 2014:840170.
78. Watanabe A, Wada Y, Obata T, et al. Delayed gadolinium-enhanced MR to determine glycosaminoglycan concentration in reparative cartilage after autologous chondrocyte implantation: preliminary results. Radiology 2006; 239:201–208.
79. Shimomura K, Hamada H, Hart DA, et al. Histological analysis of cartilage defects repaired with an autologous human stem cell construct 48 weeks postimplantation reveals structural details not detected by T2-mapping MRI. Cartilage 2021; 13(1_suppl):694S–706S.
80. Zibetti MVW, Baboli R, Chang G, et al. Rapid compositional mapping of knee cartilage with compressed sensing MRI. J Magn Reson Imaging 2018; 48:1185–1198.
81. Zhou Y, Pandit P, Pedoia V, et al. Accelerating T1ρ cartilage imaging using compressed sensing with iterative locally adapted support detection and JSENSE. Magn Reson Med 2016; 75:1617–1629.
82. Huang C, Graff CG, Clarkson EW, et al. T2 mapping from highly undersampled data by reconstruction of principal component coefficient maps using compressed sensing. Magn Reson Med 2012; 67:1355–1366.
83. Wang N, Badar F, Xia Y. Resolution-dependent influences of compressed sensing in quantitative T2 mapping of articular cartilage. NMR Biomed 2020; 33:e4260.
84. Madelin G, Chang G, Otazo R, et al. Compressed sensing sodium MRI of cartilage at 7T: preliminary study. J Magn Reson 2012; 214:360–365.
85. Knoll F, Raya JG, Halloran RO, et al. A model-based reconstruction for undersampled radial spin-echo DTI with variational penalties on the diffusion tensor. NMR Biomed 2015; 28:353–366.
86. Panda A, Mehta BB, Coppo S, et al. Magnetic resonance fingerprinting-an overview. Curr Opin Biomed Eng 2017; 3:56–66.
87. Sharafi A, Zibetti MVW, Chang G, et al. MR fingerprinting for rapid simultaneous T1, T2, and T1 ρ relaxation mapping of the human articular cartilage at 3T. Magn Reson Med 2020; 84:2636–2644.